Biogeosciences Discuss., 6, 6205–6247, 2009
www.biogeosciences-discuss.net/6/6205/2009/

Biogeosciences Discussions

Biogeosciences Discussions is the access reviewed discussion forum of *Biogeosciences*

Chemolithoautotrophic production mediating the cycling of the greenhouses gases N_2O and CH_4 in an upwelling ecosystem

L. Farías[1], C. Fernández[1,2], J. Faúndez[1], M. Cornejo[1], and M. E. Alcaman[1]

[1]Laboratorio de Procesos Oceanográficos y Clima (PROFC), Departamento de Oceanografía and Centro de Investigación Oceanográfica en el Pacífico Suroriental (COPAS), Universidad de Concepción, Casilla 160-C, Concepción, Chile
[2]Laboratoire d'Océanographie biologique de Banyuls, Université Paris VI, CNRS UMR 7621BP44, 66651 Banyuls-sur-Mer Cedex, France

Received: 19 May 2009 – Accepted: 20 May 2009 – Published: 30 June 2009

Correspondence to: L. Farías (lfarias@profc.udec.cl)

Published by Copernicus Publications on behalf of the European Geosciences Union.

Abstract

Coastal upwelling ecosystems with marked oxyclines (redoxclines) present high availability of electron donors that favour chemoautotrophy, leading in turn to high N_2O and CH_4 cycling associated with aerobic NH_4^+ (AAO) and CH_4 oxidation (AMO). This is the case of the highly productive coastal upwelling area off Central Chile (36° S), where we evaluated the importance of total chemolithoautotrophic vs. photoautotrophic production, the specific contributions of AAO and AMO to chemosynthesis and their role in gas cycling. Chemoautotrophy (involving bacteria and archaea) was studied at a time-series station during monthly (2002–2009) and seasonal cruises (January 2008, September 2008, January 2009) and was assessed in terms of dark carbon assimilation (CA), N_2O and CH_4 cycling, and the natural C isotopic ratio of particulate organic carbon (δ^{13}POC). Total Integrated dark CA fluctuated between 19.4 and 2.924 mg C m^{-2} d^{-1}. It was higher during active upwelling and represented on average 27% of the integrated photoautotrophic production (from 135 to 7.626 mg C m^{-2} d^{-1}). At the oxycline, δ^{13}POC averaged −22.209‰; this was significantly lighter compared to the surface (−19.674‰) and bottom layers (−20.716‰). This pattern, along with low NH_4^+ content and high accumulations of N_2O, NO_2^- and NO_3^- within the oxycline indicates that chemolithoautotrophs and specifically AA oxydisers were active. Dark CA was reduced from 27 to 48% after addition of a specific AAO inhibitor (ATU) and from 24 to 76% with GC7, a specific archaea inhibitor, indicating that AAO and maybe AMO microbes (most of them archaea) were performing dark CA through oxidation of NH_4^+ and CH_4. AAO produced N_2O at rates from 8.88 to 43 nM d^{-1} and a fraction of it was effluxed into the atmosphere (up to 42.85 μmol m^{-2} d^{-1}). AMO on the other hand consumed CH_4 at rates between 0.41 and 26.8 nM d^{-1} therefore preventing its efflux to the atmosphere (up to 18.69 μmol m^{-2} d^{-1}). These findings show that chemically driven chemoautotrophy (with NH_4^+ and CH_4 acting as electron donors) could be more important than previously thought in upwelling ecosystems and open new questions concerning its future relevance.

BGD

6, 6205–6247, 2009

1 Introduction

Coastal upwelling regions, most of which associated with eastern boundary current systems, significantly influence oceanic biogeochemistry in terms of marine productivity and atmospheric chemistry. Although they represent less than 1% of the area of the ocean, these areas provide about 20% of the global fish catch (Pauly and Chistensen, 1995) and give off intense N_2O and CH_4 emissions (Law and Owens, 1990; Owens et al., 1991; Nevinson et al., 2004). Physical forcing (through favourable wind stress) generally explains most biological production (Rykaczewski and Checkley, 2008) by bringing nutrient-rich water from below the pycnocline to the surface layer, boosting phytoplankton production. Nutrients supply to the surface in terms of new nitrogen (NO_3^-) co-occurs with high organic matter production or "new" production (Eppley, 1989).

The formation of planktonic biomass in such highly productive marine areas results in O_2 consumption as organic matter (OM) respiration takes place thoughout the water column. In O_2 deficient waters and sediments, O_2 concentrations act as chemical forcing (or redox gradient) for micro-organisms and, therefore, for important biogeochemical processes (Pimenov and Neretin, 2006). At the redoxcline, NH_4^+ is released during OM decomposition as well as NO_2^-, HS^- and CH_4 are being produced as NO_3^-, $SO_4^=$ and CO_2 are used as electron acceptors for anaerobic OM respiration. They can also encounter different fates but most likely, they are being used as electron donors for chemolithoautotrophic microbes processing carbon (C) in dark conditions. Although the presence of dark CO_2 assimilation or chemoautotrophic activity, has been observed in a variety of marine environments associated with redoxclines such as in the Cariaco Basin (Taylor et al., 2001), the Black Sea (Pimelov and Neretin, 2006), the Baltic Sea (Jost et al., 2008), fjords (Zopfi et al., 2001), and hydrothermal vents (both in free and episymbiont micro-organisms; Lein et al., 1997; Campbell et al., 2003), it has not been well reported in highly productive coastal upwelling ecosystems.

BGD
6, 6205–6247, 2009

Among the chemosynthetic community, nitrifying bacterioplankton (namely aerobic NH_4^+ and NO_2^- oxidizers, AAO and ANO, respectively) tranform NH_4^+ and NO_2^- to NO_3^- as a means of securing the reducing power to synthesize OM from CO_2 (Ward et al., 1989), whereas methanotrophic micro-organisms are distinguished by their ability to use CH_4 as their reducing power and sole source of carbon (Schubert et al., 2006). Both NH_4^+ and CH_4 oxidizing microbes are obligate aerobic chemolithoautotrophs. They play a central role in the biogeochemical cycles of carbon and nitrogen, not only because they produce OM and recycle bio-elements, but also because they mediate the cycling of the powerful greenhouse gases N_2O and CH_4, both of which play roles in the depletion of stratospheric ozone through photochemical reactions (Crutzen, 1991). These trace gases contribute with about 6% and 15% of the greenhouse effect, respectively (IPCC, 2001) and while the aerobic NH_4^+ oxidation "AAO" favours N_2O efflux the aerobic CH_4 oxidation "AMO" reduces CH_4 efflux into the atmosphere.

The coastal ecosystem off Central Chile presents intense upwelling during austral spring and summer (70% of the year) due to favorable wind stress (Cornejo et al., 2007). The seasonal intensification of the south and southwest winds results in the upwelling of Equatorial Subsurface Water (ESSW) with high preformed NO_3^- and low O_2 concentrations, arriving at the surface (Sobarzo and Djurfeldt, 2004). The width of the continental shelf provides a large surface area for bio-elemental exchange and benthic-pelagic coupling in subsurface waters that can reach the surface via upwelling processes. The most significant consequences of this coastal upwelling is the fertilization of the photic zone, which sustains high primary production (3–20 $g\,C\,m^{-2}\,d^{-1}$, Daneri et al., 2000; Farías et al., 2004) and outgassing of N_2O (Cornejo et al., 2007). During late autumn and early winter, on the other hand, Sub-Antarctic Water (SAAW), high in dissolved O_2 and low in nutrients, occupies the uppermost part of the water column and northernly winds predominate, driving strong and efficient vertical mixing of the water column. In this period, the coastal area acts as a N_2O sink (Cornejo et al., 2007).

This area has shallow and intense O_2 (oxycline) and nutrient (nutricline) gradients. The presence of O_2-poor waters generates an O_2 and electron donor downward flux

(associated with the active breakdown of OM produced in the surface layer). Also, the intense mineralization of OM produced in the water and sediment generates an upward flux of electron donor such as HS^-, CH_4, and NH_4^+, offering a substantial substrate for the existence of autotrophic mechanisms other than photosynthetic in the water column, which in turn, drive intense nutrient and gas recycling.

This study aims to explore the existence of important alternative autotrophic processes acting in the C and N cycling of the continental shelf waters off Central Chile, the aerobic ammonium and methane oxidizing pathways. By evaluating these chemosynthetic processes, we will attempt to answer the following questions: What is the relative importance of chemo- vs. photo-autotrophic production? Are nitrifying and methanotrophic activities significantly involved in dark C assimilation? Are AAO and AMO responsible for N_2O and CH_4 cycling in the coastal upwelling area off Central Chile?

2 Materials and methods

2.1 Site description and sampling strategy

Field work was carried out at the time series Station 18 (36°30.8′ S; 73°07.75′ W). This is located 18 nautical miles from the coast (92 m depth) over the widest continental shelf off Chile (ca. 3066 km^2) and lies between the Bio Bio and Itata submarine canyons (Fig. 1). Monthly cruises at Station 18 (L/C Kay-Kay, Universidad de Concepción) have been carried out since August 2002 as part of the time series program of the Centre for Oceanographic Research in the eastern South Pacific (COPAS) in order to identify physical and biological variability in this upwelling ecosystem. Hydrographic data (temperature, salinity, O_2, fluorescence, light) were obtained from the water column using a CTD-O_2 probe (Seabird 25). An optical sensor (Satlantic) was attached to a CTDO. Water samples were collected at 2, 5, 10, 15, 20, 30, 40, 50, 65, and 80 m depth (and sometimes at 90 m) using Niskin bottles (10 L) attached to a rosette sampler. Gases (O_2 and N_2O) and nutrients (NH_4^+, NO_3^-, NO_2^- and PO_4^{3-}) measurements were routinely

BGD
6, 6205–6247, 2009

performed. In situ autotrophic carbon assimilation rates and CH_4 measurements were included in this programme in early 2007. Determination of natural abundance of C isotopes in POC started in late 2007.

In addition to the ongoing time series programme, three seasonal process-oriented cruises were performed in order to assess specific pathways of chemoautotrophic processes: NICCHEX I (January 2008) and MI-LOCO I (January 2009) in upwelling periods and NICCHEX II (September 2008) in a non-upwelling period. During these cruises, water samples were taken from the oxycline (set at 30 m depth) and near-bottom water (set at 80 m in order to avoid the effect of particulate OM re-suspension) for biological incubation. The samples were used for light and dark C assimilation and N_2O and CH_4 time course experiments.

2.2 Field measurements

2.2.1 Chemical and geochemical analyses

During this study, samples for gas analysis were taken in triplicate. Dissolved O_2 (125 mL sample) was analyzed with an automatic Winkler method (AULOX Measurement System) developed at PROFC-Universidad de Concepción. N_2O (20 mL sample) was analyzed by creating 5 mL of He headspace equilibration in the vial and then quantifying the N_2O with a gas chromatograph (Varian 3380) using an electron capture detector maintained at 350°C connected to an auto sampler device (for more details, see Cornejo et al., 2007). CH_4 (20 mL sample) was manually analyzed on a gas chromatograph with Flame ionization detector (Schimadzu 17A) through a capillary column GS-Q (0.53 mm×30 m) with 30°C oven temperature and 4 mL min^{-1} column flow. Previously, the seawater sample was equilibrated to 40°C within 5-mL He headspace.

Dissolved NH_4^+ was determined immediately after sampling, whereas samples for dissolved NO_2^-, NO_3^- and PO_4^{3-} were filtered (0.7 μm, GF-F glass filter) on board and stored frozen until analysis. Concentrations of NO_2^-, NO_3^-, and PO_4^{3-} were determined using standard manual colorimetric techniques following Grasshoff et al. (1983). The

precision of NO_3^- and NO_2^-, in terms of coefficient variation, was better than ±10% and ±3%, respectively. For NH_4^+ concentrations, samples (triplicate) were taken directly from the Niskin bottle in 50-mL Pyrex (Duran Schott) flasks. Each sample (40 mL) received 10 mL of working solutions (OPA). Samples were then stored in the dark for 2 h and analyzed using the fluorometric method (Holmes et al., 1999) and a Turner design fluorometer. The standard error of this technique was lower than ±5%.

2.2.2 In situ Carbon Assimilation (CA) rates and natural C isotopic ratio for POC

Monthly rates of light and dark CA (representing total photoautotrophic and chemoautolitotrophic production, respectively) were obtained through incubations using the ^{13}C stable isotopic technique on an in situ mooring line. Samples from different depths were labeled with ^{13}C in the form of $NaH^{13}CO_3$ (99% ^{13}C). The tracer was added at a final tracer concentration of 10% final enrichment (0.5 mL to 580 mL incubation volume). The incubations lasted ca. 10 h (samples were generally taken at dawn and put on the line before sunset) and were terminated by filtration through pre-combusted 0.7 μm glass fiber filters (12 h; 450°C). Filters were dried at 60°C for 24 h and then stored at a constant temperature until laboratory analysis by continuous-flow isotope ratio mass spectrometry (IRMS, Finnigan Delta Plus). Prior to analysis, samples were acid-fumed to remove carbonates. International standard reference material was used for all analyses (Acetanilide).

For the elemental analysis of C and N content in POM and natural ^{13}C isotopic cha-racterization, 1 L of seawater per depth was filtered through precombusted 0.7 μm glass fiber filters. IRMS sample analysis was performed as specified above. Reproducibility for ^{13}C (based on standards) was better than 0.11‰. Isotope ratios were expressed as per mil deviations of the isotopic composition of a sample from the internationally accepted standard as defined by Eq. (1):

$$\delta^{13}C(‰) = \left[R\text{sample}/R\text{s tan dart} - 1\right] \times 1000 \quad (1)$$

where R=C:^{12}C.

Light and dark CA rates were calculated following Slawyk and Collos (1984), as stated in Eqs. (2) and (3):

$$\rho \mathrm{DI}^{13}\mathrm{C} = \left[\frac{(\%R_{\mathrm{POC}} - R_n) * \left(\frac{\mathrm{POC}}{12 * V_f} \right)}{\%R_{\mathrm{DIC}}} \right] * 12 \quad (2)$$

$$\%R_{\mathrm{DIC}} = \frac{\left(\frac{V^{13}\mathrm{C}^{*13}\mathrm{DIC}}{V_b} \right) + \mathrm{DIC}_i * 0.01112}{\mathrm{DIC}_V - \frac{V^{13}\mathrm{C}^{*13}\mathrm{DIC}}{V_b}} * 100 \quad (3)$$

where V_f represents the filtered volume and POC is the amount of POC recovered in the filter after incubation and measured by mass spectrometry (μg). The excess enrichment of the tracer after inoculation (To) is indicated by $\%R_{\mathrm{DIC}}$, which is calculated using Eq. (3). The $\%R_{\mathrm{POC}}$ indicates the ^{13}C enrichment in the filter after incubation, measured by the tracer mass. In Eq. (2), V^{13}C indicates the volume of ^{13}C added to the sample during inoculation, whereas ^{13}DIC refers to the tracer concentration added to the sample (3.6456 mg ^{13}C ml^{-1}). DIC_i represents the initial amount of DIC in the sample. For this study, we used a constant value (26 mg C L^{-1}) based on previous measurements in the study area. V_b is the volume in the incubation flask (0.6 L). Because natural ^{13}C abundance data are only available for late 2007 and 2008, we used % ^{13}C abundances from the literature.

In order to determine the fraction of total dark autotrophic CA that can be associated with the aerobic NH_4^+ and CH_4 oxidizing pathways, biogeochemical experiments were performed at 30 (oxycline) and 80 m depth (near-bottom water) during NICCHEX (I and II) and MI-LOCO cruises. Seawater samples were dispensed – avoiding oxygenation – into acid cleaned 600-mL glass bottles (in duplicate or triplicate) sealed with septum caps. These were amended with three treatments: 1 – ^{13}C; 2 – ^{13}C plus allylthiourea (hereafter referred as ATU) and; 3 – ^{13}C plus N1-guanyl-1, 7-diaminoheptane (hereafter referred as GC7). Experiments were incubated in the laboratory at a similar in

situ temperature and in the dark. ATU (FLUKA), which is a specific inhibitor of the NH_4^+ monooxygenase enzyme was added at a final concentration of 86 μM final (Ginestet et al., 1998). Given the physiological and biochemical similarities between AA and AM oxidizing microbes (Hanson and Hanson, 1996), ATU may also significantly affect CH_4 cycling. GC7 (BIOSERCH), a known phylogenetic inhibitor of archaea, was added at a final concentration of 500 mM (Jansson et al., 2000) in order to inhibit the deoxyhypusine synthase enzyme and, thus, discern the group of microbes involved in CA, and N_2O and CH_4 cycling. Controls were without any inhibitor and negative controls were tested with $HgCl_2$. Incubations lasted between 13 and 24 h. and samples were filtered at three different times (t0, t1 and sometime t2), through pre-combusted glass fiber filters prior to mass spectrometry analysis (IRMS). Initial and final dissolved inorganic nitrogen concentrations were measured for each sample as described above.

2.2.3 N_2O and CH_4 cycling (aerobic NH_4^+ and CH_4 oxidation)

During the NICCHEX and MI-LOCO cruises, experimental assays were performed in the laboratory in order to evaluate the kinetics of N_2O and CH_4 cycling and to determine possible associations with chemoautotrophic activities (e.g., AAO and AMO). For this purpose, water was dispensed – avoiding oxygenation – into 1-L double-laminated aluminium-polyethylene bags. Each bag had a hose/valve with a septum through which all the different treatments were injected. A permeability test was performed prior to the experiment. The bags were filled with helium and monitored for 24 h using gas chromatography and showed no atmospheric gases (N_2O or CH_4) intrusions, therefore proving hermetically sealed. We could then confidently exclude the possibility of oxygenation during the incubation process. The cycling rate of N_2O and CH_4 over time or its accumulation or consumption was determined under natural in situ O_2 and temperature (11–13°C) conditions, without (the control) and with the addition of ATU and GC7 inhibitors (which were slowly injected into the bags through a septum with gastight syringes). Subsamples were retrieved from the bags for N_2O and CH_4 analysis at different times (one or two bags per experiment), by applying pressure on the bags; this

BGD
6, 6205–6247, 2009

water was poured into GC bottles. For each incubation time, three GC bottles with incubated water were injected with 50 μL of saturated $HgCl_2$ in order to stop all biological reactions; the bottles were then sealed with rubber stoppers and metallic caps.

The net rates of N_2O and CH_4 cycling were calculated from the slopes of the linear regressions of the concentration as a function of time for each treatment. Positive slope values represented gas accumulation and negative values indicated consumption. The rate uncertainty was calculated directly from the standard error of the slope for control, ATU and GC7 treatments. Student's t-test and ANOVA were used to evaluate the significance of slopes and the differences between the treatments.

2.3 Data analysis

The depth of the euphotic zone (irradiation at 1% of its surface value, PLD) was estimated from the attenuation coefficient of downwelling irradiance. A density-based criterion was used to determine the mixed layer depth (MLD). The equilibrium concentrations of dissolved N_2O and CH_4 were calculated according to the Weiss and Price (1980), and Weisenburg and Guinasso (1979) equations, respectively. N_2O and CH_4 flux across the air-sea interface was determined using the Eq. (4) as modified by Wanninkhof (1992):

$$F = k * \left([N_2O] - [N_2O]^*\right) \quad (4)$$

where F (μmol m^{-2} d^{-1}) is the flux across the air-sea interface, k (cm h^{-1}) is the gas transference velocity depending on wind and water temperature, $[N_2O]$ and $[CH_4]$ (nM) are the N_2O and CH_4 concentrations measured in the mixed layer, and $[N_2O]^*$ is the N_2O concentration at relative equilibrium with the atmospheric concentration. k was calculated according to Eq. (5):

$$k = 0.31^* W^{2*} \left(Sc/660\right)^{-0.5} \quad (5)$$

where Sc is the Schmidt number, the relationship between viscosity and diffusion coefficient of N_2O in water, it depends on the temperature of the seawater. The wind

BGD
6, 6205–6247, 2009

data, used to determine k, were measured at a coastal station close to the sampling area. Wind speed was recorded every hour and, for flux estimations, daily averages of the wind speed were used.

In order to interpret the O_2 and electron donor vertical distributions along with CA rates, the water column was divided into three layers corresponding to their hydrographic features: 1 – a illuminated and mixed surface layer (S-L) with high O_2 content; 2 – a middle layer associated with the oxycline (O-L), with hypoxic conditions and a strong redox gradient, extending from the depth at 1% of surface irradiance (this coincides with the base of the MLD, estimated to be the upper limit of the oxycline, to 65-m depth, coinciding with the 22 μM O_2 isocline; and 3 – a bottom layer (B-L) with very low O_2 in which CH_4, NH_4^+ and NO_2^- exist. The B-L extends from 66 m depth to the water overlying the sediments (92 m).

Integrated light and dark CA was calculated by numerically integrating (trapezoidal quadrature) the measured CA rate with respect to specific depth ranges. Integrated photosynthetic CA (light bottles) was calculated as the integrated values from the surface to the depth of 1% surface irradiance, whereas dark CA (dark bottles) were calculated by integrating rates from the surface to depth of 1% incident light (S-L) and from 1% incident light to 92 m (in the O and B layers). Hourly rates were multiplied by 12 (photo CA) or 24 (dark CA) to obtain daily rates. Gas and nutrient inventories were estimated as lineal depth integrations by layer (see depth range) from data interpolated from each meter. Correlations between environmental variables and geochemical parameters (nutrient and gas inventories) as well as between δ^{13}POC and CA rates were performed through Spearman rank correlation (ρ). The significance of ρ (p<0.05) was determined using F-test.

3 Results

3.1 Temporal variability of physical variables

The time series plots (August 2002 to date) of temperature (T°), salinity (S) and σ-t (σt) are shown in Fig. 2. The mixed layer depth (MLD) fluctuated between 2 and 20 m; whereas the depth of the photic layer (PLD) ranged between 12 and 40 m depth. The PLD varied seasonally, being shallower in summer compared to wintertime. In general, it did not match the MLD as shown in Table 1. An analysis of the vertical distribution of physical variables by layers shows that the S-L was wind-mixed, influenced by warming in summer and subjected to precipitation in the winter, resulting in highly variable temperature (11.1°< surface T<18.1°C) and salinity (28.73<surface S<34.56). The O-L extended from below 1% surface irradiance to 65 m depth (this is an arbitrary depth assumed to be uninfluenced by the sediments and in which O_2 levels are close to 22 μM). Although the temperature was less variable in this layer than in the S-layer, σt revealed a clear seasonal cycle (see Fig. 2c). This parameter indicated that the ESSW was present almost all spring, summer and early autumn, whereas the SAAW was only present during austral winter (i.e., May, June, July). The B-L was confined to depths below 65 m, where the physical components were less variable and the ESSW was in contact with the sediments most of the time.

3.2 Temporal variability of gases (O_2, N_2O and CH_4)

Time series plots for gases O_2, N_2O and CH_4, the latter only measured since April 2007, are shown in Fig. 3. Table 1 also presents the depth of the 22 μM oxycline, N_2O and CH_4 inventory by layers and their air-sea fluxes. The vertical distribution of O_2 showed clear seasonal variations and matched well with physical variables and processes. In late autumn and winter, high O_2 was observed throughout the entire water column. During this period, temperature was almost uniform, with a deeper thermocline; σt showed the presence of the SAAW in the O-L and B-L. However, in

spring-summer, O_2 decreased abruptly from the base of the thermocline, considered to be the top of the oxycline. The S-L was always well oxygenated with O_2 levels ranging between 329 and 183 μM. The O-L was subject to large O_2 fluctuations (from ~220 to ~2.81 μM). Most of the time, the 22 μM isobath lies at 60–70 m depth and marks the beginning of hypoxic conditions, forming a good separation between the O-L and B-L. It is note worthy that depth of the 22 μM O_2 lies on average at 61 m (see Table 1). The O_2 content in the B-L was low (<22 μM, and sometimes down to 1–3 μM) except in periods of strong vertical mixing (i.e., winter). These nearly anoxic conditions were mostly observed in late summer, after several upwelling events that resulted in the accumulation of a large amount of OM on the sediments produced by the sedimentation of successive phytoplanktonic blooms.

The temporal variability of the vertical distribution of N_2O (see Fig. 3b) agreed well with the temporal O_2 variation (see Fig. 3a). In winter, the S-L and O-L had low N_2O levels (<11.7 nM) and high O_2 concentrations (>180 μM). In contrast, during the upwelling favorable periods, N_2O increased and O_2 decreased in the S-L and O-L. Very high N_2O maxima (up to 244.7 nM) were observed in the O-L in summer (December 2004, March 2007, December 2008, January 2009), creating a "hotspot" (see Fig. 3b). N_2O inventories reflected such distribution, being significantly higher in this layer (in average 42.2% of total N_2O pool). The temporal variability of the B-L was higher (10.50–70.61 nM), fluctuating with relation to the O_2 fluctuations. i.e., when O_2 dropped below 10 μM, generally in late summer and early autumn, diminishing N_2O values were observed, suggesting high N_2O consumption by denitrification (see Fig. 3b).

The temporal variability of the vertical CH_4 distribution (see Fig. 3c) showed seasonal variations, peaking in upwelling favorable periods, when O_2 concentrations dropped. During these periods, the CH_4 concentration was high, especially in the bottom waters and gradually diminished towards the surface. This vertical pattern coresponded to O_2 concentrations that showed an exponential decrease with depth, and also a marked CH_4 production from the sediment and maybe even from the B-L.

The N_2O and CH_4 fluxes across the air-sea interface estimated from April 1997 to present time (see Table 1) ranged from −2.32 to 42.8 μmol m^{-2} d^{-1} and from 0.86 to 18.7 μmol m^{-2}, respectively. Both fluxes were maximal in upwelling periods (see Table 1). CH_4 inventories increased, in average, with depth from the S-L in contact with the atmosphere (in average 463.8 μmol m^{-2}) to the B-L in contact with the sediment (934.5 μmol m^{-2}), indicating that the bottom water and sediments are the most probable sources of this gas and that it is maybe being consumed in the water column as it difused upward (see Table 1). In contrast, N_2O inventories did not show an increase toward the sediment; the N_2O pool size in the O-L was higher than in the S-L and B-L in summer (up to 5.885 μmol m^{-2}; see Table 1). This pattern matches the NO_3^- and NO_2^- vertical distribution (see Table 2).

3.3 Temporal variability of N-species

Time series plots and inventories for nutrients are shown in Fig. 4 and Table 2, respectively. NH_4^+ concentrations were generally high although variability was observed. The NH_4^+ concentrations in the S-L varied from 0.1 to 3.2 μM (Fig. 4a). Interestingly, this range is greater than values obtained in the O-layer, in which low concentrations were always observed. Bottom waters (B-L) had the highest concentrations of NH_4^+ (up to 8.5 μM) in summer as the sediments can act as a source of NH_4^+ (Farias et al., 2004). On average, 25% of the total NH_4^+ pool was present in the O-L, whereas S-L contained between 50% and 95.6% (equivalent to 35.55 mmol m^{-2}).

Nitrite showed a marked fluctuation in the study area, ranging from 0.1 to 11 μM. The S-layer presented moderate and almost constant NO_2^- content, whereas the O-L showed a very wide range of NO_2^- concentrations. This layer had a lower average NO_2^- inventory (27%) than the S-L and B-L (40.4 and 32.4%, respectively). However, NO_2^- levels and inventories reached maxima in summer (up to 3 μM, 160.17 mmol m^{-2}; January 2008), and were accompanied by higher N_2O and NO_3^- concentrations, suggesting N_2O production by AAO (see Fig. 4b, Table 2). In the B-L, the NO_2^- content

was also very variable, ranging between 0.5 and 11 μM (Fig. 4b). As with NH_4^+, a fraction of the NO_2^- might come from the sediments, but some may also be produced by nitrification and denitrification processes that could be acting in the B-L at O_2 deficient levels.

Nitrate concentrations were always high during our study, being the most abundant oxidized N-compound in the water column. The NO_3^- concentrations were never depleted in the S-L, even in periods associated with high photoautotrophic production (see below). Within the O-L, NO_3^- levels were variable, ranging from 14.5 to 35.7 μM, and showed seasonal patterns, i.e., enhanced NO_3^- during upwelling-favorable periods and diminished NO_3^- during non-upwelling periods. This variation agrees with the presence of these water masses (see Fig. 2b) but, at the same time, NO_3^- concentrations as high as 35 μM (coinciding with the N_2O and NO_2^- hotspot described above) indicate that nitrification is an active process occurring in this layer. In fact, the NO_3^- and also N_2O inventory peaked in the O-layer in upwelling periods (December 2007, December 2008), where high NO_3^- and N_2O pool sizes, up to 1.586 mmole m^{-2} and 5.885 μmol m^{-2}, respectively, were measured. In the B-L, NO_3^- concentrations were lower than expected according to the presence of the ESSW (with high pre-existing nitrate levels). This indicates significant NO_3^- consumption in the bottom water or from the sediments (e.g., March 2008).

3.4 Carbon assimilation rates, POC content, and its C isotopic composition

Temporal variations of light and dark CA rates (ρ^{13}C), and the δ^{13}POC and POC contents are shown in Fig. 5. Simultaneous estimations of photo- and dark CA, POC content, and its isotopic composition and areal daily photo and dark CA rates through S-L and O-L plus B-L are presented in Table 3. The photo CA rate (ρ^{13}C) varied between 0.20 and 825 mg C m^{-3} d^{-1} and maximum rates were observed at the surface (2 m depth) during upwelling favorable periods (December 2007, October 2008, January 2009; see Fig. 5a). Dark CA activity (ρ^{13}C) or chemoautotrophic

production was (although one order of magnitude lower than the rates of photoautotrophic production values) surprisingly high in term of CA. In the photic zone (S-L), dark CA rates fluctuated between 0.20 and 145 mg C m^{-3} d^{-1} (see Table 3) and maximum rates were observed at the subsurface (15–30 m depth). In the O-L and B-L (non photic zone), dark CA fluctuated from 0.16 to 117 mg C m^{-3} d^{-1} and was slightly higher in the B-L near the sediments than in the O-L (see Fig. 5b). As with photosynthetic activity, chemosynthetic activity was always higher during upwelling favorable periods (i.e., December 2007, January 2009). In the S-L, daily integrated rates ($\sum \rho^{13}$C) for photoautotrophic production ranged between 0.135 and 7.626 mg C m^{-2} d^{-1}, while daily integrated rates for chemoautotrophic production fluctuated from 8.06 to 2.851 mg C m^{-2} d^{-1}. In the O-L and B-L (or aphotic zone) daily integrated rates of dark CA were 11.3–1802 mg C m^{-2} d^{-1}. On average, half of chemoautotrophic production came from the S-L (although values as high as 94% were observed in April 2008), whereas the other half of the dark CA was concentrated in the O-L and B-L (see Table 3).

POC concentration varied between 59.1 and 1.282 mg m^{-3}. The POC content decreased exponentially from the surface to the middle layer and then increased slightly towards the bottom. The POC concentration was remarkably high in the S-L (see Fig. 5d). This distribution was a persistent feature and correlated well with the bacterioplankton distribution, which showed maximal abundance in both the surface and bottom water (Galan et al., 2009). The C:N ratio in the POM was around 5.5–8 (data not shown), and increased with depth (i.e., the B-L). The C:N ratio indicated that the produced OM is typically marine in origin and diagenesis or sediment resuspension could have minor effect on the C:N ratio of the collected POM. δ^{13}POC was highly variable (16.930 to −28.595‰), although the water column was only 92 m in depth (see Fig. 5d). The vertical distribution of δ^{13}POC revealed an important vertical zonation that could reflect the influence of C metabolic processes and environmental conditions. In the S-layer, the mean value of δ^{13}POC was −19.674‰; this was subject to low variation (±2.206‰ SD). In the O-layer, the mean value of δ^{13}POC decreased to

−22.209‰ and temporal variation was higher between months (±2.75‰ SD). This variation was reflected in a range from −17.752‰ to values to as depleted as −28.594‰ (see Fig. 5d, December 2007). These lighter δ^{13}C-POC values were accompanied by high NO_3^- , NO_2^- and N_2O during summer, e.g., December 2007, January 2008. The average of δ^{13}POC in the B-layer was 20.716‰. The mean δ^{13}POC differed significantly among layers (t-student, $p<0.05$), but when differentiating between non-and upwelling periods, further differences were found between layers.

In the O-L, the N- oxides inventories (N_2O, NO_2^- and NO_3^-), but not NH_4^+ showed higher and significant correlations with dark CA (ρ=0.57 p=0.0008, ρ=0.299 p=0.028 and ρ2=0.5 p=0.002, respectively); whereas NH_4^+ more than the N-oxides (except NO_3^-) presented an important correlation with dark CA rate in the B-L (ρ=0.39 p=0.02). The strong correlation with N-species inventories and dark CA rate in the O and B-layer indicate that exists chemical energy to chemolithoautotrophic production via nitrification, while in the S-L, photo CA rates are subjected to rapid nutrient and C turnover driven largely by light energy, which, in turn, was not possible reflect trough the inventories and CA correlation. CH_4 inventory was inversely correlated with dark CA within the O-L.(ρ=−0.58 p=0.02)

3.5 Dark carbon assimilation and N_2O and CH_4 cycling associated with AAO and AMO

Table 4 shows the results of experiments carried out in the O-L and O-L along with other environmental conditions measured at these sampling times. Figure 6 shows a representative time course for the accumulation of POC and N_2O and CH_4 cycling experiments performed at Station 18, using a control (without any addition) and ATU and GC7 inhibitor experiments. ATU should inhibit NH_4^+ and CH_4 oxidation and, therefore, may diminish dark CA, N_2O production and CH_4 consumption due to the inhibition of their monooxygenase systems. In contrast, GC7 acts on archaeal nitrifying and methanotrophs and, therefore, on their metabolic pathway associated with CA and

N_2O and CH_4 cycling.

The accumulation of POC in dark ^{13}CA experiments was linear over time (see Fig. 6a) and rates ranged from 0.21 to 4.91 mg C m^{-3} d^{-1}, peaking in January 2009 (MI-LOCO cruise, see Table 4). These rates were of the same order of magnitude as in situ monthly incubations. Dark CA was effectively reduced by 28 to 48% with ATU (estimated by average rates; see Table 4). The effect of GC7 on archeal CA was most obvious in the B-L, unlike that of ATU. Dark CA rates decreased up to 76% in the B-layer. Overall, dark CA rates were higher in samples amended with ATU inhibitor compared to GC7 (average 25 and 51% higher at 30 and 80 m depth, respectively; see Table 4).

CH_4 was consumed in both layers at rates fluctuating between 0.41 and 26.83 nM d^{-1}. CH_4 consumption was highest at the B-L. In contrast, N_2O accumulated in both layers throughout the experiment. This means that N_2O is produced at rates of 8.88 to 43.0 nM d^{-1}, the highest rates being observed in upwelling periods and in the O-L. ATU had a significant effect on gas cycling (see Table 4). In the case of CH_4, its consumption increased, but less production was measured for N_2O cycling (see Table 4). GC7 had also an effect on net gas cycling. For N_2O, the use of GC7 reduced the accumulation of N_2O. For CH_4 on the contrary, this inhibitor increased three and ten-fold its consumption rate.

4 Discussion

The continental shelf water off Central Chile is one of the most productive marine ecosystems in the world, sustaining the highest primary and fisheries productivity in the global ocean. This high productivity is usually explained by the coastal upwelling process that brings subsurface, nutrient-rich waters to the surface. This process is driven by the winds and fertilizes the surface waters, promoting phytoplankton blooms and the transfer of matter and energy to higher trophic levels and towards the surface sediments (Escribano et al., 2004; Farías et al., 2004). The observed high magnitude

and temporal variability of biological productivity in this system, however, cannot be explained solely by the effect of physical factors related to the onset of the upwelling process. The presence of high dark CA, which has been also observed in some redoxclines (e.g., Zopfi et al., 2001), was explored during this study as a possible explanation for such variability.

Oxygen is undoubtly a chemical forcing factor in this coastal upwelling ecosystem because the tight link between its vertical distribution and its consumption due to respiration of sinking POM, which is enhanced by upwelling events in the austral spring-summer. The vertical distribution of nutrients and gases also reflects the seasonality of C cycling, which in turn, strongly affects the microbial ecology and geochemistry of most coastal ecosystems. Carbon cycling via photoautotrophic activity can be clearly seen through the concentrations of NH_4^+, NO_2^-, and CH_4 which were highest during upwelling favorable periods and remained present mostly in the B-L year round.

It is known that all reduced species can act as electron donors for dark CA or chemolithoautotrophic processes. To determine how much chemical energy is acting in these systems, pool sizes were estimated for measured reduced species assuming that NH_4^+, NO_2^- and CH_4 oxidation are occurring in the area with O_2 as the electron acceptor. Electron donor inventories for each layer were estimated by linear depth integration for each predefined layer. These inventories (see Table 2) were then converted into chemical energy, taking into account Gibbs free energy (ΔG°). This means the enthalpy of a reaction (ΔH) of different electron donors with O_2 as an electron acceptor, assuming that these electron donors are completely oxidized by the O_2 in the water column. The ΔG° from AAO, ANO and AMO are −274.7, −74.1 and 890 Kj mol^{-1} (Madigan, 2003). These reactions sum in total −295.7 Kj m^{-2} for the study period which is a large amount of chemical energy in terms of kjoules per mol of oxidized species. Most of the chemical energy (about 70%) comes from NH_4^+ oxidation during upwelling favorable periods, although the oxidation of Fe and S species (not considered in this estimation) could be important in the area.

BGD
6, 6205–6247, 2009

4.1 What is the relative importance of chemo- vs. photo-autotrophic production?

Chemosynthesis is the non-photosynthetic biological conversion of C1 molecules (usually CO_2 or CH_4) into OM. Figure 7 shows the integrated photo vs. chemoautolithotrophic production in the whole water column. Integrated rates of chemoautotrophic CA were as high as 2.924 gC m^{-2} d^{-1} and they represented on average 29% (maxima of 98% in October 2007 and 2008) of the integrated photoautotrophic production (up to 7.626 gC m^{-2} d^{-1}). Dark CA rates in the photic layer reached between 0.3 and 37% of surface photoautotrophic production (see Table 3). Dark CA rates in the aphotic zones or O-L and B-L (excluding the photic layer) were as high as 1.802 gC m^{-2} d^{-1} (see Table 3). These values suggest the existence of a large pool of organic matter of chemosynthetic origin that has not been accounted for this or other coastal upwelling ecosystems.

In other redox systems, e.g., the Black Sea, Cariaco basin and the Baltic Sea, dark CA rates of up to 2.1, 30, and 18 mg C m^{-3} d^{-1} have been reported (Pimenov and Neretin, 2006; Taylor et al., 2001; Jost et al., 2008). In the Black Sea, integrated chemosynthetic rates in the range of 300–800 mg C m^{-2} d^{-1} were measured, and accounted for 50–80% of primary production; whereas in the Carriaco basin dark CA represented on average 70% of primary production. Likewise, in the Mariader fjord, dark CA accounted for 37% of total C fixation, but rates were as high as 1.092 mg C m^{-3} d^{-1}, leading to the possibility of an important heterotrophic CA activity within a narrow chemocline (Zopfi et al., 2001) Our rates fall in the hightest range of these measurements (for comparison see Table 5). Nevertheless, it is important to note that those systems are euxinic environments where chemolithoautotrophy is fuelled by reduced S-species. In contrast, the upwelling area off Central Chile does not seem to involve sulphide utilization (HS^- levels seem to be < μmolar) but exhibit large NH_4^+ levels, often on the μmolar scale. In addition, sediments underlying upwelling off Central Chile had low pore water HS^- concentrations (<2 μM) but held high $SO_4^=$ reduction rates (Tham-

BGD
6, 6205–6247, 2009

drup and Canfield, 1996). This pattern has not been explained yet; while Jørgensen and Gallardo (1999) argue by the presence of *Thioploca*, the massive mat-forming, large nitrate-storing and sulfide-oxidizing bacteria, Thamdrup and Canfield (1996) suggest that metals could be acting as important oxidizing agents.

These results combine well with our evidence and could indicate that the chemolithotrophic community is gaining sufficient energy by oxidizing N-compounds but not so rapidly as they are being produced, thereby visible NH_4^+ accumulations are observed (see Fig. 4a, b). The strong correlations found between N oxidazed species inventories and dark CA rates, but not with NH_4^+ confirm that nitrification is one who is consuming NH_4^+ and producing N_2O, NO_2^-, and NO_3^-. In this sense, the absence of HS^- in this system, that can act as a powerful inhibitor at high concentrations of nitrification (Joyce and Hollibough, 1995), could explain the high chemolithoautotrophic activity measured and also high observed nitrifying activities (up to 90 nM d^{-1}; C. F. Fernández, personal communication, 2009).

The results also revealed a significant vertical variation of δ^{13}POC, in spite of continuous water column mixing due to vertical advection (summer time) or turbulent mixing (winter time) and the sinking of OM from the surface to the bottom and chemotrophic activity, mostly associated with the oxycline. The oxycline has a strong isotopic C signal on OM (reaching values as light as −28.594‰) and it is significantly lighter than those signals from the S-L (reaching values as hevier as −16.934‰). This means that, if OM from photosynthetic phytoplankton is being oxidized as it sinks, its isotopic signal should reflect its origin. However, the O-L was characterized by a distinct isotopic composition. In fact, chemosynthetic organisms generally result in greater use of the lighter isotope and, as a result, the chemosynthetically produced C has a more negative isotopic composition than that C of photosynthetic origin (Fry et al., 1991; Hayes, 2001). According to the above, the observed vertical pattern (see Fig. 5c) suggests chemoautotrophic production leading to predominantly OM produced in situ. A similar pattern was found by Coban-Yildiz et al. (2006) in the Black Sea. The C:N vs. δ^{13}Corg-POM diagram lead us to exclude the possibility of terrestrial influence, de-

spite the closeness of our station to the coast (18 nm) and is on the continental shelf, receiving high fresh water discharges from the Bio Bio River, mostly in winter time.

According to the time series data on dark CA, rates were often higher at the base of the euphotic zone, though fixation was constantly detected at all depth levels and coincided in space and time with photoautotrophic production. This distribution recalls the classic description of nitrification in coastal areas, a process not only able to oxidize NH_4^+ to NO_2^- but also able to fix C via nitrifying bacteria (Ward et al., 1989). In this study, we used the stable isotope ^{13}C in contrast to the commonly used radioactive carbon isotope ^{14}C, which has been widely used for estimating nitrification and dark CA. However, the use of ^{13}C reduces the incompatibilities in time scales of biological activity and the experimental setup; ^{14}C studies often include non-biological dark CA (Markager, 1998).

4.2 Are nitrifying and methanotrophic activities significantly involved in dark C assimilation?

Total bacterial abundances (measured by flow cytometry) can reach 4×10^6 cell mL^{-1} in surface waters and 1×10^6 cell mL^{-1} in near-bottom waters during upwelling favorable periods (G. A. Alarcón and O. U. Ulloa, personal communication, 2009). Archaea also represent a significant fraction of the total prokaryotic community off Central Chile. They can account for about 50% in terms of abundance at the bottom and up to 25% in the surface waters of our study area (Levipan et al., 2007a; Quiñones et al., 2009). The general abundance of archaea has been estimated to be close to 5×10^5 cells mL^{-1} at 80 m depth and chrenarchaeota, one of the most important groups involved in chemolithoautotrophic NH_4^+ oxidation, could potentially reach 30% of the total prokaryotic community based on DAPI counting (L. B. Belmar, personal communication, 2009).

The GC7 inhibitor used in this study is known to affect archaeal (and possibly eukaryote) protein synthesis (Janson et al., 2000) and has been used in the past to ex-

plore the significance of methanogenic archaea at the time series Station 18 (Levipan et al., 2007b). We investigated archaeal (CG7 sensitive) and NH_4^+ or CH_4 oxidizing bacteria (ATU sensitive) groups through our dark ^{13}CA experiments and gas cycling (see Table 4). The results confirm their presence and proved them capable of CA in dark conditions at the oxycline and near-bottom depth level (and also are involved in gas cyling, see below). Using inhibitors, we obtained rates of ATU sensitive microbes as AAO and AMO bacteria of around half the values associated with the archaeal groups (1.27 vs. 0.6 mg C m^{-3} d^{-1}). This experimental approach suggests then the occurrence of archaeal and bacteria chemolithoautotrophic microbes in the same experimental samples. Taking into account the reported abundance of each group at 80 m depth, we estimated a CA rate of around 63 fg $cell^{-1}$ d^{-1} for archaea and around 60 fg $cell^{-1}$ d^{-1} for bacteria. The average C content of prokaryotic microorganisms previously reported in the study area is ~43 fg $cell^{-1}$ (Levipan et al., 2007a), indicating the capacity of chemosynthetic production to meet the daily C demand of chemoautotrophic C fixers, at least during the spring-summer period. Additionally, the calculated specific rates of dark CA, ranged from 0.005 up to 0.05 h^{-1}, reflect the existence of an active, relatively rapidly growing chemoautotrophic community, whose components have yet to be determined.

Although we are in no position to evaluate the importance of a specific pathway (AAO and AMO), the availability of substrates such as NH_4^+ and CH_4 in the water column suggest that most of this dark CA occurs by their oxidation. Specific rates (h^{-1}) in both cases changed dramatically with the addition of ATU or GC7 compared to total dark CA. When excluding ATU-sensitive NH_4^+ and CH_4 oxidizers, the specific CA rates were lower than the specific CA obtained when excluding archaeal microbes. This suggests that the chemosynthetic C utilization per unit of POC per time is sensitive to the community structure and archaeal C fixers are important players in the C turnover of the system. We can, therefore, expect a variable but important proportion of active prokaryotes co-existing year-round with an equally variable photoautotrophic community.

BGD
6, 6205–6247, 2009

Until now, very little effort has been done to distinguish dark CA from different group of microbes. Some advances were performed in Black sea, where most of them are bacteria associated with the S-cycle and concentrated at the redoxcline (Pimenov and Neretin, 2006). In the Namibian cost (~23° S) chemolithotrophic bacteria affiliated to γ- and ϵ-proteobacteria, accounting for approximately 20% of the bacterioplankton in sulphidic waters, can create a buffer zone between the toxic sulphidic subsurface waters and the oxic surface waters (Lavik et al., 2009). In our study area, about 10% of the microbial afilation has been identified as thiotrophic microbes (O. U. Ulloa, personal communication, 2009). Our results then add to the role of N-species as important chemical-driven factors and propose further questions regarding S and N species interaction.

4.3 N_2O and CH_4 cycling and effluxes towards the atmosphere in a coastal upwelling area off Central Chile

It is now recognized that the oceans are an important source of N_2O (Nevison et al.,1995; Bange et al., 1996), accounting for 20 to 25% of natural N_2O sources ($15\,Tg\,N_2O\,y^{-1}$; Nevison et al., 1995). Aerobic NH_4^+ oxidizers and NO_2^- reducers (denitrifiers) are the main producers of N_2O. In the case of CH_4, the oceans are responsible for about 8% of the global emissions from natural sources, accounting for approximately $15\,Tg\,y^{-1}$ of CH_4 (Owens et al.,1991; Bange, et al., 1996) but it is believed that methanotrophs consume up to 90% of the CH_4 produced by the ocean, significantly reducing the CH_4 emission into the atmosphere (Crutzen, 1991).

Our estimated N_2O fluxes ranged from -2.32 to $42.85\,\mu mol\,m^{-2}\,d^{-1}$ and confirmed that the study area is an important source of N_2O to the atmosphere during upwelling favourable periods, with values similar to those reported by Cornejo et al. (2007) and for other areas of high biological productivity, e.g., the Arabian Sea (Law and Owens 1990). In the case of CH_4, effluxes were estimated to be between 0.86 and $18.69\,\mu mol\,m^{-2}\,d^{-1}$. Although little information exists for CH_4 fluxes in upwelling areas,

the CH_4 efflux rates off Central Chile were very high compared to published values for the Arabian Sea (Owens et al., 1991; Upstill-Goddard et al., 1999) but could be even higher if methanotrophs did not act. The marked seasonal cycling in both fluxes confirms that vertical advection by coastal upwelling is the main outgassing mechanism.

Net CH_4 cycling rates were negative in both O-L and B-L, indicating that CH_4 is being consumed (see Table 4). However, in the B-L, CH_4 was consumed at a lower rate (see Table 4), suggesting that methanogenesis also could be acting in the same layer. However, the lack of an adequate resolution in the water column and the difficulty of measuring processes and gas cycling rates near the sediments precludes determining the source of CH_4. Among methanotrophic or CH_4 consuming microbes, the anaerobic CH_4 oxidizer archaea in consortium with sulphate reducing bacteria remove a large fraction of CH_4 (Schubert et al., 2006). However, given the predominance of hypoxic conditions, the high afinity of methane mono-oxygenase enzime for O_2 (0.1–16 μmol L^{-1}, Trotsenko and Murrell, 2008) and the response of net CH_4 cycling rates to ATU inhibition, AMO is the most likely process using CH_4. These results re-open the question about the co-occurrence of CH_4 and NH_4^+, even if one single group can oxidize either CH_4 or NH_4^+ (Poret-Peterson et al., 2008).

Net N_2O cycling rates were positive in both layers indicating that N_2O is being produced (see Table 4). Four main pathways have been described leading to N_2O production (Farias et al., 2009); they are partial denitrification, or NO_2^- reduction to N_2O; nitrite-ammonification, the conversion of NO_3^- to NH_4^+; nitrification, including NH_4^+ oxidation to NO_2^- and nitrifier denitrification. But so far, only one process – total denitrification – is known to consume N_2O, i.e. N_2O reduction to N_2, under extremely low O_2 (<4.4 μM) or suboxic conditions (Elkins et al., 1978; Farías et al., 2009). Thus, the amount of N_2O in the ocean depends on a balance of N_2O production and consumtion processes. The prevalence of N_2O accumulation in all the experiments indicates that production processes are predominant. The reduction of N_2O cycling rates in experiments treated with ATU (see Table 4) suggests that NH_4^+ oxidation is one of these N_2O-producing processes in the study area. Not total reduction of net N_2O accumulation by ATU in-

dicates that N_2O is also being produced by denitrification (NO_2^- reduction to N_2O), but its total reduction to N_2 is not discarded in the B-L, where O_2 levels are too low to allow complete denitrification. Although NH_4^+ oxidation and CA rates are coherent with reported NH_4^+ oxidizing activities, there are no further elements to allow an assesment of the potential contribution of other NH_4^+ oxidizers or even other potentially ATU-sensitive communities (e.g., aerobic methanotrophs). On the other hand, N_2O cycling and dark CA rates were also reduced in GC7 amended experiments providing the most direct evidence of the presence of NH_4^+ oxidizing archaea are active in the study area.

5 Summary

Our study reveals that dark CA fixation within the redoxcline of the coastal area off Central Chile sustains a fraction of the in situ biological production observed, mainly as a result of autotrophic nitrifying and methane oxidation. Increased chemoautotrophic activity as a response to upwelling favourable periods can in turn explain more N_2O effluxes (associated with nitrifying activities) but less CH_4 effuxes (associated with methanotrophic activities). In the long term, these results have important environmental implications because of the leading role of O_2 in controlling OM dynamics through heterotrophic or autotrophic processes.

Hypoxia is a well-known feature in major eastern boundary currents where coastal upwelling occurs (Helly and Levin, 2004). The development of severe hypoxia has been reported by Naqvi et al. (2000) in the Arabian Sea and by Grantham et al. (2004) in the northeast Pacific. Mechanisms for these events are different; one is explained by increased eutrophication and the other by changes in oceanic currents, both of these are being influnced by global climate change (Deutsch et al., 2005; Stramma et al., 2008). An expected consequence is the expansion of O_2 deficient waters, the decrease in O_2 solubility because of the warming of the surface-layer could account for much of the enhanced O_2 depletion in the upper ocean. Increases in temperature imply a thermal stress higher, which could lead to stronger winds and therefore upwelling persistence

(Bakum, 1990). The possible responses of coastal ecosystems include changes in the microbial community structure and diversity, and strong biogeochemical transformations (in two of the main known biogeochemical processes nitrification and photosynthesis) affecting atmospheric-oceanic exchanges of carbon and nitrogen (as CO_2 and N_2O). Therefore, if hypoxic conditions intensify in the world ocean, the importance of chemical energy would be translated into a highly active chemosynthetic community.

Acknowledgements. This research was funded by the FONDECYT Grant #1070518 and partially by the Gordon and Betty Moore Foundation (MI-LOCO I cruise). We thank the captain and crew of the Kay Kay research vessel and colleagues who facilitated our observations and sample collection, as well as Mauricio Gallegos and Jamey Redding for assisting with the IRMS and field analyses, respectively. Once again, we are thankful to Antony Davies for improving the English of the text and Osvaldo Ulloa for critical reviews of this manuscript.

References

Bakum, A.: Global climate changes and the intensification of coastal upwelling, Science, 241, 148–201,1990.

Bange, H., Rapsomanikis, S., and Andreae, M. O.: Nitrous oxide in coastal waters, Global Biogeochem. Cy., 10, 197–207, 1996.

Campbell, B., Stein, J. L., and Cary, C.: Evidence of Chemolithoautotrophy in the Bacterial Community Associated with Alvinella pompejana, a Hydrothermal Vent Polychaete, Appl. Environ. Microb., 69, 5070–5078, 2003.

Coban-Yildiz, Y., Altabet, M. A., Yilmaz, A., and Suleyman, S.: Carbon and nitrogen isotopic ratios of suspended particulate organic matter (SPOM) in the black Sea water columns, Deep-Sea Res. Pt. II, 53, 1875–1892, 2006.

Cornejo, M., Farías, L., and Gallegos, M.: Seasonal variability in N_2O levels and air-sea N_2O fluxes over the continental shelf waters off Central Chile (~36° S), Progr. Oceanogr., 75, 383–395, 2007.

Crutzen, P. J.: Methane's sink and source, Nature, 350, 380–391, 1991.

Daneri, G., Dellarossa, V., Quiñones, R. A., Jacob, B., Montero, P., and Ulloa, O.: Primary pro-

duction and community respiration in the Humboldt Current System off Chile and associated oceanic areas, Mar. Ecol.-Prog. Ser., 197, 41–49, 2000.
Deutsch, C., Emerson, S. R., and Thompson, L.: Fingerprints of climate change in North Pacific oxygen, Geophys. Res. Lett., 32, L16604, doi:10.1029/2005GL023190, 2005.
Elkins, J. W., Wofsy, S. C., Mcelroy, M. B., Kolb, C., and Kaplan, W. A.: Aquatic sources and sinks for nitrous oxide, Nature, 275, 602–606, 1978.
Eppley, R. W.: New production: history, methods, problems, in: Productivity of the ocean: present and past, edited by: Berger, W. H., Smetacek, V. S., and Wefer, G., John Wiley & Sons Limited, Chichester, New York, 85–97, 1989.
Escribano, R., Daneri, G., Farías, L., Gallardo, V. A., González, H. E., Gutierrez, D., Lange, C. B., Morales, C. E., Pizarro, O., Ulloa, O., and Braun, M.: Biological and chemical consequences of the 1997–1998 El Niño in the Chilean coastal upwelling system: a synthesis, Deep-Sea Res., 51, 2389–2411, 2004.
Farías, L., Castro-González, M., Cornejo, M., Charpentier, J., Faúndez, J., Boontanon, N., and Yoshida, N.: Denitrification and nitrous oxide cycling within the upper oxycline of the oxygen minimum zone off the eastern tropical South Pacific, Limnol. Oceanogr., 54, 132–144, 2009.
Farías, L., Graco, M., and Ulloa, O.: Nitrogen cycling in continental shelf sediments of the upwelling ecosystem off Central Chile, Deep-Sea Res. pt. II, 51, 2491–2505, 2004.
Fry, B., Jannasch, H. W., Molyneaux, S. J., Wirsen, C. O., Muramoto, J. A., and King, S.: Stable isotope studies of the carbon, nitrogen ans sulfur cycles in the Black Sea and Cariaco trench, Deep-Sea Res., 38, S1003–S1019, 1991.
Galan, A., Molina, V., Thamdrup, B., Woebken, D., Lavik, G., Kuypers, M., and Ulloa, O.: Anammox bacteria and the anaerobic oxidation of ammonium in the oxygen minimum zone off northern Chile, Deep-Sea Res. Pt. II, 56, 1125–1135, 2009.
Ginestet, P., Audic, J., Urbain, V., and Block, J.: Estimation of nitrifying bacterial activities by measuring oxygen uptake in the presence of the metabolic inhibitors Allylthiourea and Azide, Appl. Environ. Microb., 64, 2266–2268, 1998.
Grantham, B. A., Chan, F., Nielsen, K., David, S., Fox, D. S., Barth, J. A., Huyer, A., Lubchenco, J., and Menge, B. A.: Upwelling-drivennearshore hypoxia signals ecosystem and oceanographic changes in the northerm Pacific, Nature, 429, 749–754, 2004.
Grasshoff, K., Ehrhardt, M., and Kremling, K.: Methods of seawater analysis, Springer Verlag, Basel, Switzerland, 2nd edn., 419 pp., 1983.
Hanson, R. and Hanson, T. E.: Methanotrophic Bacteria, Microb. Rev., 60, 439–471, 1996.

Hayes, J. M.: Fractionation of carbon and hydrogen isotopes in biosynthetic processes, in: Stable isotope geochemistry, edited by: Valley, J. W. and Cole, D. R., Rev. Mineral Geochem., 43, 225–278, 2001.
Helly, J. and Levin, L.: Global distribution of naturally occurring marine hypoxia on continental margins, Deep-Sea Res., 51, 1159–1168, 2004.
Ho, T-Y., Taylor, G., Astor, Y., Varela, R., Taylor, G. T., and Scranton, M. I.: Vertical and temporal variability of redox zonation in the water column of the Cariaco: implications for organic carbon oxidation pathways, Mar. Chem., 86, 89–104, 2004.
Holmes, R. M., Aminot, A., Kérouel, R., Hooker, B. A., and Peterson, B. J.: A simple and precise method for measuring ammonium in marine and freshwater ecosystems, Can. J. Fish. Aquat. Sci., 56, 1801–1808, 1999.
IPCC: Climate Change: The Scientific Basis, edited by: Houghton, J. T., Ding, Y., Griggs, D. J., Noguer, M., van der Linden, P. J., Dai, X., Maskell, K., and Johnson, C. A., Cambridge University Press, 2001.
Janson, P. B. M, Malandrin, L., and Johansson, H.: Cell cycle arrest in Archea by the Hypusination inhibitor N^1-Guanyl-1,7-Diaminoheptane, J. Bacteriol., 182, 1158–1161, 2000.
Jørgensen, B. B. and Gallardo, V. A.: *Thioploca* spp.: Filamentous sulfur bacteria with nitrate vacuoles, FEMS Microbiol. Ecol., 28, 301–313, 1999.
Jost, G., Zubkov, M. V., Yakushev, E., Labrenz, M., and Jurgens, K.: High abundance and dark CO_2 fixation of chemolithotrophic prokaryoyes in anoxic water of the Baltic Sea, Limnol. Oceanogr., 53, 14–22, 2008.
Joyce, S. B. and Hollibaugh, J. T.: Influence of sulfide inhibition of nitrification on nitrogen regeneration in sediments, Science, 270, 623–625, 1995.
Labrenz, M., Jost, G., Pohl, C., Beckmann, S., Martens-Habbena, W., and Jürgens, K.: Impact of Different In Vitro Electron Donor/Acceptor Conditions on Potential Chemolithoautotrophic Communities from Marine Pelagic Redoxclines, Appl. Environ. Microb., 71, 6664–6672, 2005.
Lavik, G., Stührmann, T., Brüchert, V., Van der Plas, A., Mohrholz, V., Lam, P., Mußmann, M., Fuchs, B. M., Amann, R., Lass, U., and Kuypers, M. M. M.: Detoxification of sulphidic African shelf waters by blooming chemolithotrophs, Nature, 457, 581–584, 2009.
Law, C. S. and Owens, N. J. P.: Significance flux of atmospheric nitrous oxide from the northwest Indian Ocean, Nature, 346, 826–828, 1990.
Lein, A. Y., Pimenov, N. V., and Galchenko, V. F.: Bacterial chemosynthesis and methanotrophy

in the Manus and Lau basis ecosystems, Mar. Geol., 142, 47–56, 1997.
Levipan, H. A., Quiñones, R. A., and Urrutia, H.: A time series of prokaryote secondary production in the oxygen minimum zone of the Humboldt Current System. Prog. Oceanogr., 75, 531–549, 2007a.
Levipan, H. A., Quiñones, R. A., Johansson, H. E., and Urrutia, H.: Methylotrophic Methanogens in the Water Column of an Upwelling Zone with a Strong Oxygen Gradient Off Central Chile, Microbes Environ., 22, 268–278, 2007b.
Madigan, M., Martinko, J., and Parker, J.: Brock Biology of Microorganism. Nutrition and Metabolism, Prentice Hall, New Jersey, 10th edn., 1011 pp, 2003.
Markager, S.: Dark uptake of inorganic ^{14}C in oligotrophic oceanic waters, J. Plankton Res., 20, 1813–1836, 1998.
Naqvi, S. W. A., Jayakumar, D. A., Narvekar, P. V., Naik, H., Sarma, V. V., D'Souza, W., Joseph, S., and George, M. D.: Increased marine production of N_2O due to intensifying anoxia on the Indian continental shelf, Nature, 408, 346–349, 2000.
Nevison, C. D., Weiss, R. F., and Erickson, D. J.: Global oceanic emissions of nitrous oxide, J. Geophys. Res., 100, 15 809–15 820, 1995.
Nevison, C. D., Lueker, T. J., and Weiss, R. F.: Quantifying the nitrous oxide source from coastal upwelling, Global Biogeochem. Cy., 18, GB1018, doi:10.1029/2003GB002110, 2004.
Owens, N. J. P., Law, C. S., Mantoura, R. F., Burkill, P. H., and Llewellyn, C. A.: Methane flux to the atmosphere from the Arabian Sea, Nature, 354, 293–296, 1991.
Pauly, D. and Christensen, V.: Primary production required to sustain global fisheries, Nature, 374, 255—-257, 1995.
Pimenov, N. V. and Neretin, L.: Composition and activities of microbial communities involved in carbon, sulfur, nitrogen and manganese cycling in the oxic/anoxic interface of the Black Sea, in: Past and present Water Column Anoxia, edited by: Neretin, L. N., NATO Science Series IV: Earth and Environmental Sciences, 501–502, 2006.
Poret-Peterson, A. T., Graham, J. E., Gulledge, J., and Klotz, M. G.: Transcription of nitrification genes by the methane-oxidizing bacterium, Methylococcus capsulatus strain Bath, ISME Journal, 2, 1213–1220, 2008.
Quiñones, R. A., Levipan, H. A., and Urrutia, H.: Spatial and temporal variability of planktonic archaeal abundance in the Humboldt Current System off Chile, Deep-Sea Res. Pt. II, 56, 1083–1092, 2009.
Rykaczewski, R. R. and Checkley Jr., D. M.: Influence of ocean winds on the pelagic ecosystem

in upwelling regions, P. Natl. Acad. Sci. USA, 105, 1965–1970, 2008.
Schubert, C. J., Coolen, M. J. L., Neretin, N. L., and Schippers, A.: Aerobic and anaerobic methanotrophs in the Black Sea water column, Environ. Microbiol., 8, 1844–1856, 2006.
Sobarzo, M. and Djurfeldt, L.: Coastal upwelling process on a continental shelf limited by submarine canyons, Concepción, Central Chile, J. Geophys. Res., 109, C12012, doi:10.1029/2004JC002350, 2004.
Slawyk, G. and Collos, Y.: ^{13}C and ^{15}N uptake by marine phytoplankton III. Interactions in euphotic zone profiles of stratified oceanic areas, Mar. Ecol.-Prog. Ser., 19, 223–231, 1984.
Stramma, L., Johnson, G. C., Sprintall J., and Mohrholz, V.: Expanding Oxygen-Minimum Zones in the Tropical Oceans, Science, 320, 655–658, 2008.
Taylor, G. T., Iabichella, M., Tung-yuan, H., Scranton, M., Thunell, R., Muller-Karger, F., and Varela, R.: Chemoautotrophy in the redox transition zone of the Cariaco Basin: A significant midwater source of organic carbon production, Limnol. Oceanogr., 46, 148–163, 2001.
Trotsenko, Y. A. and Murrell, J. C.: Metabolic aspects of aerobic obligate methanotrophy, Adv. Appl. Microbiol, 63, 183–229, 2008.
Thamdrup, B. and Canfield, D. E.: Pathway of carbon oxidation in the continental margin off Central Chile, Limnol. Oceanogr., 41, 1629–1650, 1996.
Upstill-Goddard, R. C., Barnes, J., and Owens, N. J.: Nitrous oxide and methane during the SW mosoon in the Arabian Sea/northwestern Indian Ocean, J. Geophys. Res., 104, 30 067–30 084, 1999.
Wanninkhof, R.: Relationship between wind speed and gas exchange over the ocean, J. Geophys. Res., 97, 7373–7382, 1992.
Ward, B. B., Glover, H. E., and Lipschultz, F.: Chemoautotrophic activity and nitrification in the oxygen minimum zone off Peru, Deep-Sea Res., 36, 1031–1051, 1989.
Weiss, R. F. and Price, B. A.: Nitrous oxide solubility in water and seawater, Mar. Chem., 8, 347–359, 1980.
Weisenburg, D. A. and Guinasso, N. L.: Equilibrium solubilities of methane, carbon monoxide and hydrogen in water and seawater, J. Chem. Eng. Data, 24, 354–360, 1979.
Zopfi, J., Ferdelman, T. G., Jorgensen, B. B., Teske, A., and Thamdrup, B.: Influence of water columns dynamics on sulfide oxidation and other major biogeochemcial processes in the chemoline of Mariager Fkord (Denmark), Mar. Chem., 74, 29–51, 2001.

Table 1. Physical and chemical properties of the water column and nitrous oxide and methane content by layer (expressed as inventories) and their fluxes across air-sea interface at Station 18 during April 2007–January 2009.

Time series cruise	Mixed layer depth	Photic layer depth	Depth 22 μM oxycline	Nitrous oxide					Methane				
				Inventory [N_2O]			air-sea flux	Surface N_2O [CH_4]	Inventory			air-sea flux	Surface CH_4
	m	m	m	μmol m^{-2}				nM	μmol m^{-2}				nM
				S-L	O-L	B-L			S-L	O-L	B-L		
Apr 2007	10	45	63	834	611.6	805.6	6.87	−0.88	122.8	828.1	998.3	14.60	5.20
May 2007	17	40	69	517.1	610.3	820.4	7.63	−0.59	599.8	480.3	1275	12.58	3.89
Jun 2007	20	45	89	635.2	468.4	680.8	8.79	−0.21	786.9	410.1	870.4	18.80	3.75
Jul 2007	2	31	74	3892	929.2	951.1	14.10	0.88	189.9	241.0	142.6	6.53	0.86
Aug 2007	1	36	79	628.3	748.4	924.1	15.56	1.44	697.3	821.0	1181	20.09	4.58
Sep 2007	15	23	90	321.0	846.9	788.1	13.17	0.56	364.9	824.1	651.9	16.16	2.32
Oct 2007	7	10	90	226.5	1881	984.1	17.75	2.14	147.5	818.8	736.7	13.14	2.90
Dec 2007	4	10	31	233.0	2464	1545	16.57	3.84	133.3	628.3	492.1	12.36	5.30
Jan 2008	8	14	14	447.9	4400	2157	30.11	15.13	386.5	2486	1699	27.65	18.69
Feb 2008	2	34	50	815.9	1131	1268	13.71	0.62	540.0	710.9	936.3	13.56	1.37
Mar 2008	9	41	63	878.8	1043	1672	14.30	2.72	540.0	649.1	1226	12.52	5.16
Apr 2008	5	32	59	755.7	1290	946.5	14.30	2.18	652.4	573.2	850.7	19.92	8.11
May 2008	6	33	86	404.5	511.8	645.3	11.70	0.99	289.6	545.5	761.0	11.86	4.42
Jun 2008	13	47	57	n.m.	855.5	n.m.	5.60	−2.32	944.0	758.4	1439	7.81	3.18
Sep 2008	6	44	66	1553	1309	1633	21.74	6.33	423.7	320.8	944	7.23	2.48
Oct 2008	4	16	73	404.8	1684	994.5	22.5	5.52	230.9	952.2	646.6	11.36	3.82
Nov 2008	7	15	19	653.8	3222	1578	35.4	16.81	115.2	585.2	824.2	7.58	3.34
Dec 2008	5	26	33	2419	5885	1286	75.3	42.85	398.1	1153	1175	17.84	10.13
Jan 2009	14	12	47	269.1	1936	1405	19.60	6.36	143.8	699.8	905.5	10.05	5.19
Average[b]	8.1	29.1	61	703.9	1675	1113	21.31	5.49	463.8	762.4	934.5	13.77	4.98

[a] Gray color indicates favorable upwelling period. n.m.: not measured. [b] average among months (n=19). S-L: comprised from surface to 1% irradiance. O-L: comprised from <1% surface irradienace to 65 m depth. B-L: comprised from 66 m depth to bottom.

Table 2. Ammonium, nitrite and nitrate inventories (mmol m^{-2}) and their content percent (%) by layer at Station 18 during April 2007–January 2009.

Time series cruise	Ammonium inventory mmol m^{-2}						Nitrite inventory mmol m^{-2}						Nitrate inventory mmol m^{-2}					
	S-L	O-L	B-L	% S-L*	% O-L*	% B-L*	S-L	O-L	B-L	% S-L[c]	% O-L[c]	% B-L[c]	S-L	O-L	B-L	% S-L[c]	% O-L[c]	% B-L[c]
Apr 2007	n.d.	n.d.	n.d.	n.d.	n.d.	n.d.	15.09	0.74	1.28	88.18	4.33	7.50	1295.	709.8	904.7	44.52	24.39	31.09
May 2007	15.05	6.37	6.75	53.44	22.60	23.97	8.68	0.96	0.78	83.31	9.17	7.52	106.5	534.4	761.5	45.08	22.65	32.28
Jun 2007	n.d.	n.d.	n.d.	n.d.	n.d.	n.d.	16.02	1.34	8.03	63.09	5.28	31.63	113.8	688.3	906.8	41.68	25.17	33.16
Jul 2007	19.60	2.37	0.50	87.22	10.55	2.22	21.90	6.62	0.50	75.47	22.80	1.72	499.1	793.6	581.6	26.63	42.34	31.03
Aug 2007	13.02	6.13	2.49	60.17	28.33	11.50	11.36	12.48	2.80	42.65	46.84	10.51	605.8	613.5	487.1	35.50	35.95	28.55
Sep 2007	n.d.	n.d.	n.d.	n.d.	n.d.	n.d.	6.39	12.13	7.03	24.99	47.49	27.52	282.6	916	629.9	15.46	50.10	34.45
Oct 2007	n.d.	n.d.	n.d.	n.d.	n.d.	n.d.	2.60	3.07	1.83	34.65	40.92	24.43	237.1	1621	847.3	8.76	59.92	31.32
Dec 2007	23.06	35.27	10.25	33.62	51.43	14.95	1.24	8.48	13.65	5.31	36.29	58.41	107.1	1586	755.5	4.37	64.78	30.85
Jan 2008	10.52	11.85	7.77	34.91	39.31	25.78	5.07	160.17	140.42	1.66	52.40	45.94	249.8	1309	489.6	12.20	63.90	23.90
Feb 2008	7.20	0.73	1.80	74.04	7.46	18.51	17.62	2.09	7.00	65.96	7.83	26.21	790.4	903.5	664.1	33.52	38.32	28.16
Mar 2008	5.24	0.24	0.25	91.44	4.19	4.37	13.17	0.96	2.58	78.80	5.74	15.46	656.5	599.8	360.6	40.60	37.10	22.30
Apr 2008	35.55	0.98	0.65	95.62	2.64	1.74	11.33	6.78	8.58	42.44	25.40	32.16	740.9	896.7	682.5	31.93	38.65	29.42
May 2008	32.06	32.65	69.20	23.94	24.38	51.68	14.93	17.06	13.68	32.69	37.36	29.96	582.6	607.1	580.5	32.91	34.30	32.79
Jun 2008	n.d.	n.d.	n.d.	n.d.	n.d.	n.d.	12.76	0.91	26.60	31.69	2.25	66.06	994.6	479.2	542.9	49.32	23.76	26.92
Sep 2008	8.55	0.98	12.15	39.42	452	56.06	6.08	0.56	4.22	55.98	5.16	38.86	738.6	525.9	660.2	38.38	27.32	34.30
Oct 2008	8.88	2.00	9.37	43.85	46.27	46.27	0.82	4.07	6.27	7.39	36.44	56.17	67.99	1195.9	627.7	3.59	63.22	33.18
Nov 2008	14.04	14.40	18.18	30.12	30.88	39.00	1.95	14.79	13.35	6.48	49.15	44.37	157.1	1380.3	608.1	7.32	64.33	28.34
Dec 2008	4.49	101.12	98.61	2.20	49.52	48.28	14.71	108.04	132.34	5.77	42.35	51.88	444.9	828.6	333.8	27.68	51.55	20.77
Jan 2009	14.32	10.39	8.73	42.82	31.07	26.11	2.30	3.94	4.28	21.90	37.46	40.64	112.9	1267.3	668.9	5.51	61.85	32.64
Average[d]	15.11	16.10	17.62	50.92	25.22	26.46	26.46	26.46	26.46	40.44	27.09	32.47	566.7	918.8	636.5	26.58	43.66	29.76

[c] Percentage of each layer with respect of total pool size of the whole water column. [d] Averange of values among months from April 2007 to January 2009.

BGD
6, 6205–6247, 2009

Table 3. Values of carbon assimilation (range and integrated values) and natural C isotopic ratio for S- and O-layer + Bottom layer at Station 18 during April 2007–January 2009.

	S-Layer					O + B-Layer				Total water column[e]
Time serie cruises	Photo ρ^{13}C range	Dark ρ^{13}C range	Photo $\sum\rho^{13}$C	Chemo $\sum\rho^{13}$C	δ^{13}Corg	Dark ρ^{13}C range	Dark $\sum\rho^{13}$C	δ^{13}Corg O-L	δ^{13}Corg B-L	Dark $\sum\rho^{13}$C
	mg m^{-3} d^{-1}	mg m^{-3} d^{-1}	mg m^{-2} d^{-1}	mg m^{-2} d^{-1}	‰[f]	mg m^{-3} d^{-1}	mg m^{-3} d^{-1}	‰	‰	mg m^{-2} d^{-1}
Apr 2007	69.9–96.4	0.30–0.46	2521	10.95	n.d.	0.24–0.38	15.5			26.40
May 2007	44.8–125	0.28–0.39	2514	9.69	n.d.	0.20–0.24	13.0			22.7
Jun 2007	66.3–91.3	0.20–0.25	2402	11.20	v.d.	–	–			–
Jul 2007	56.3–144	0.24–0.32	2901	8.06	n.d.	0.16–0.32	11.3			19.4
Aug 2007	1.83–123	1.43–2.14	1203	53.77	n.d.	0.53–2.35	87.6			141
Sep 2007	0.65–366	n.d.	3411	n.d.	n.d.	n.d.	n.d.			–
Oct 2007	19.2–25.9	6.25–12.5	232	87.54	−21.550	0.45–0.62	142	−24.631	−22.277	230
Dec 2007	149–404	70.2–84.9	4428	1149	−17.206	1.17–6.23	807	−24.861	−21.957	1956
Jan 2007	–	–	–		−17.821	–	–	−19.817	−19.507	–
Feb 2008	0.42–173	0.92–3.27	2093	78.94	−22.288	0.63–0.99	58.6	−24.026	−20.877	138
Mar 2008	2.75–80.9	0.90–2.33	1290	53.39	−22.645	0.40–0.50	26.4	−23.067	−21.620	79.8
Apr 2008	0.16–75.6	0.28–15.7	1748	235.7	−18.977	0.38–0.74	16.0	−19.670	−21.292	264
May 2008	0.75–13.5	0.38–1.55	135	23.18	−24,956	0.54–1.51	51.4			49.62
Jun 2008	0.58–42.1	0.42–0.87	549	19.56	−25,477	0.49–0.66	27.3			46.8
Sep 2008	1.61–274	0.22–1.31	4295	21.08	−22.381	–	–	−25.020	−23.863	2.62
Oct 2008	224–435	29.9–44.0	6805	725.8	n.d.	1.24–101	1802	n.d.	n.d.	2527
Nov 2008	46.7–200	32.5–38.4	1387	109.1	−17.644	1.22–70.0	991	−20.355	−20.830	1351
Dec 2008	2.81–134	1.23–4.92	1590	109.1	−19742	1.16–1.46	67.0	−19.113	−18.361	185
Jan 2009	0.75–825	0.66–145	7626	2851	−17.942	1.24–1.86	71.7	−20.637	−19.499	2924

[e] Total dark CA in the whole water column (integration from surface to 92 m depth). [f] Average for each time series cruise that include samples taken from S-layer (n=2–4). ** average that include samples taken form O-layer (n=2–3), *** average that include samples taken from B-layer, n=2–3. n.d. not determinated.

BGD
6, 6205–6247, 2009

Table 4. Rates of dark Carbon assimilation (mg C m^{-3} d^{-1}) and N_2O and CH_4 (nM d^{-1}) recycling along with environmental conditions at the O- and B-layer.

Cruises	NICCHEX I		NICCHEX II		MI-LOCO I	
Layer depth	O-layer 30 m	B-layer 80 m	O-layer 30 m	B-layer 80 m	O-layer 30 m	B-layer 80 m
Date	Jan 2008	Jan 2008	Sep 2008	Sep 2008	Jan 2009	Jan 2009
Enviromental variables						
Temperature (°C)	10.5	10.2	11.4	10.3	10.5	10.5
O_2 (ml/L)	0.14	0.07	3.34	0.30	1.63	0.04
NH_4 (μM)	0.12	1.04	0.04	0.10	0.31	0.40
N_2O (nM)	62.1	49.6	23.5	40.3	31.4	19.6
CH_4 (nM)	41.5	132.7	9.44	40.6	9.14	37.1
C Metabolims rate (mgC m^{-3} d^{-1})						
Dark C assimilation rate	n-d	3.53±1.40	0.24±0.04	0.21±0.04	0.49±1.13	4.91±0.77
Dark C assimilation+ATU	n-d	2.54	n-d	0.18±0.05	0.44±0.03	2.54±0.17
Dark C assimilation+GC7	n-d	0.47	n-d	0.16±0.06	0.36±0.04	1.31±0.41
% Microbes sensitive to ATU	n-d	27.88	–	14.3	10.21	48.0
% Microbes sensitive to GC7	n-d	76.33	–	24.8	26.54	73.3
Gas cycling (nM d^{-1})						
[g] Net N_2O	40.05±3.55 32.37±1.51	23.36±0.58 22.01±1.57	8.88±2.88	16.80±6.00	22.41±2.93	42.96±8.76
N_2O+ATU	30.05±5.35		5.21±.85	13.27±1.56	13.81±3.84	7.22±2.90
N_2O+GC7	25.32±5.24	11.42±3.37	n-d	n-d	n-d	n-d
[g] Net CH_4	−1.60±0.55 −3.00±1.20	−0.41±0.07 −1.32±0.82	n-d	−1.68±0.72	−5.30±2.88	−26.83±8.16
CH_4+ATU	−7.68±0.96	n-d	n-d	−1.78±0.41	−18.00±2.4	−23.76±6.24
CH_4+GC7	n-d	−13.26±0.50		n-d	n-d	−91.20±7.44

[g] two bags by experiment.

Table 5. Literature and present estimates of chemolithotrophic rates in the main redoxclines.

Area	Dark CA rates mg C m^{-3} d^{-1}	Cell abundance cell mL^{-1}	Method	Source
[h]The Black sea	0.45–2.10 (0.11–0.20) 0.30–0.8	1.5–5.5×10^5 (1)	^{14}C	Pimelov and Neretin (2006), Sorokin fide Pimelov and Neretin (2006)
[i]The Baltic sea	2.40–18.0 8.4–16.8	1.16-1.65×10^6 (2)	^{14}C 1^4C in vitro	Jost et al. (2008), Labrenz et al. (2005)
[j]Cariaco Basin	0.5–30 2.4–31.2 (0.32–1.90)	1.9–7.4×10^5 (1)	^{14}C	Taylor et al. (2001), Ho et al. (2004)
[k]Mariager Fjord	115.5–1092 (0.12)	not measured		Zopfi et al. (2001)
Central Chile shelf water	0.16–70 (0.02–2.92)	5.X 10^5–4X10^6 (2)	^{13}C	This study

Values in parenthesis are integrated rates (g m^{-2} d^{-1}).
[h] Gotland Deep and Landsort Deep; rates measured at redoxcline (100–300 m depth), not O_2 but HS^- was detected.
[i] Gotland Deep and Landsort deep, redoxcline at 120–150 m.
[j] Cariaco Basin 10° 50′ N; 64°66′ W; redoxcline at 240–450 m depth HS^- accumulation up to 40 μmol L^{-1}.
[k] Mariager Fjord (Denmark) 56° 39′ N; 09° 58′ E. 25 m depth; rates measured at redoxcline (13–15 m), HS^- as high as 75 μmol L^{-1} was measured.
(1) DAPI counting; (2) flow cytometry counting.

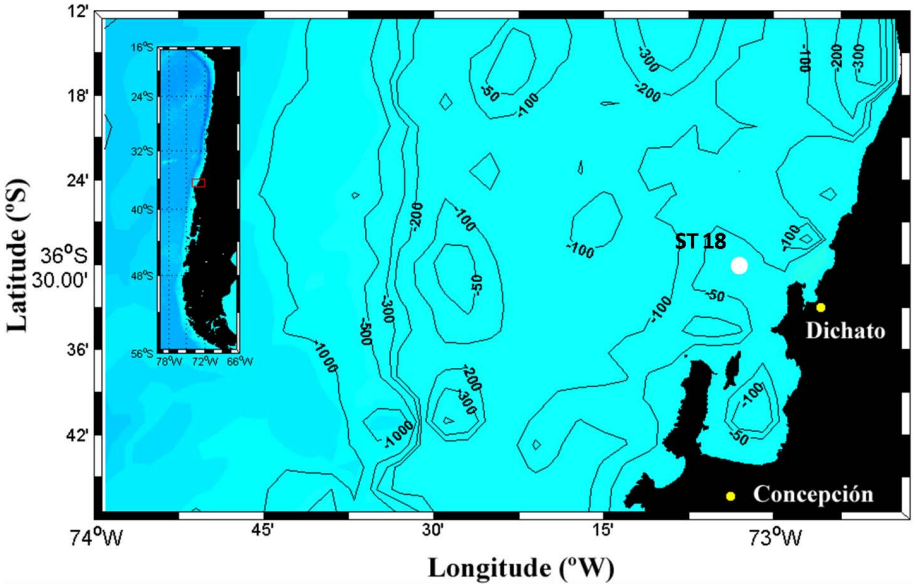

Fig. 1. Map showing the location of Station 18 (36°30.80′ S–73°07.75′ W) occupied monthly by the COPAS oceanographic center for physical-chemical-biological integrated time series study since August 2002. The Central Chile continental shelf is delimited the north and south by two submarine canyons. Bathymetric contours are in meters.

BGD
6, 6205–6247, 2009

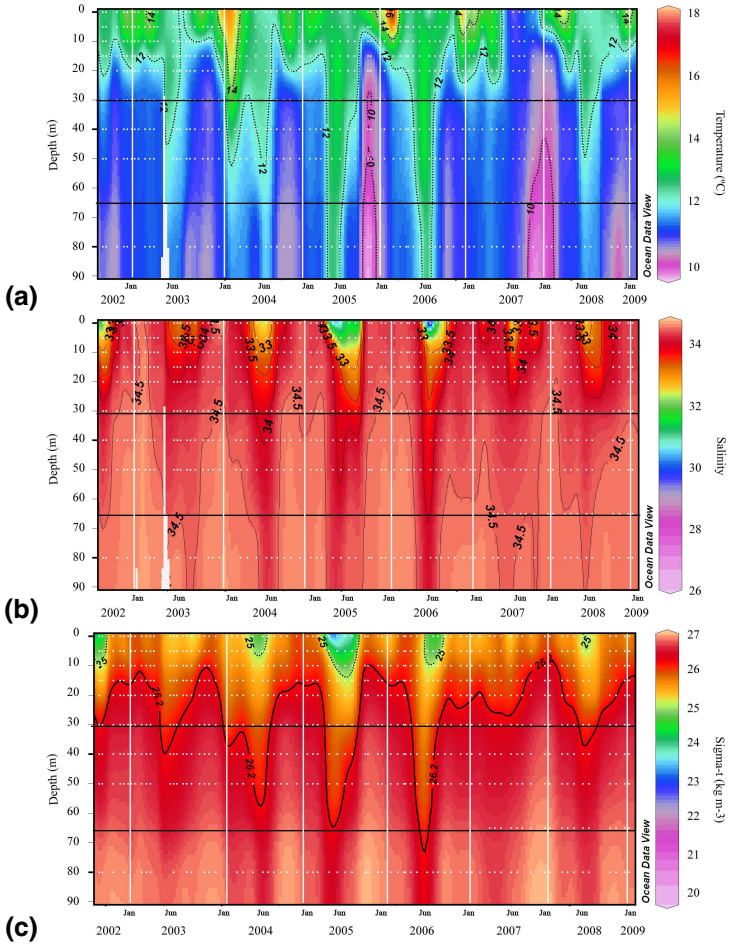

Fig. 2. Temporal variability of temperature **(a)**, salinity **(b)**, and density **(c)** at Station 18 (August 2002 to date). Horizontal lines separate the predetermined layers. 26.2 σt set the presense of the ESSW.

BGD
6, 6205–6247, 2009

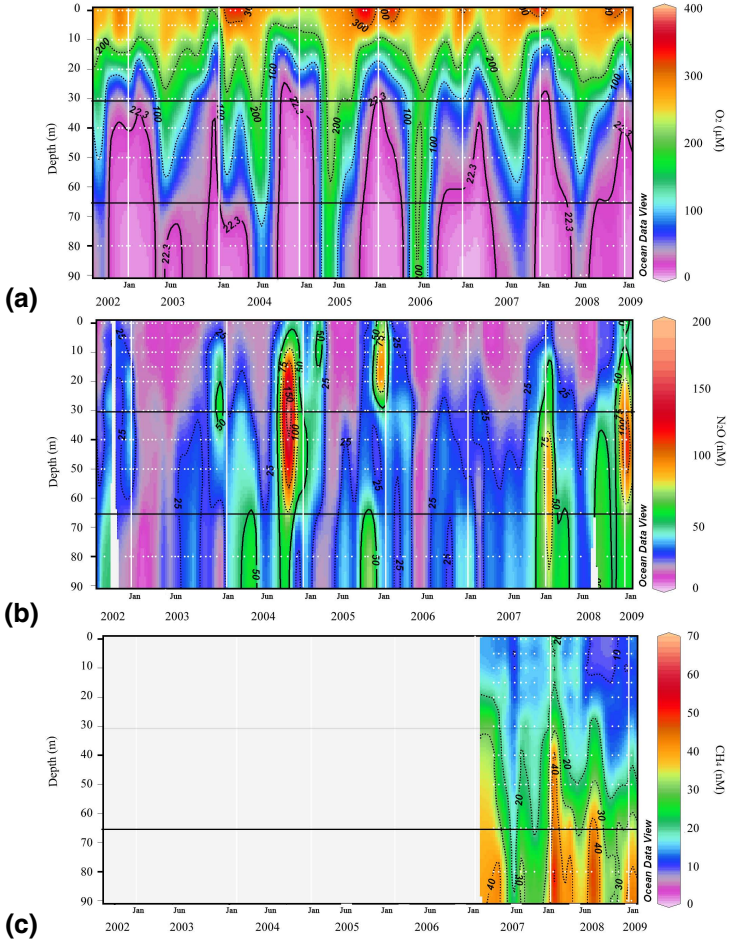

Fig. 3. Temporal variability of **(a)** oxygen, **(b)** nitrous oxide, and **(c)** methane concentration at Station 18 (August 2002 to date). CH_4 (data since April 2007).

BGD
6, 6205–6247, 2009

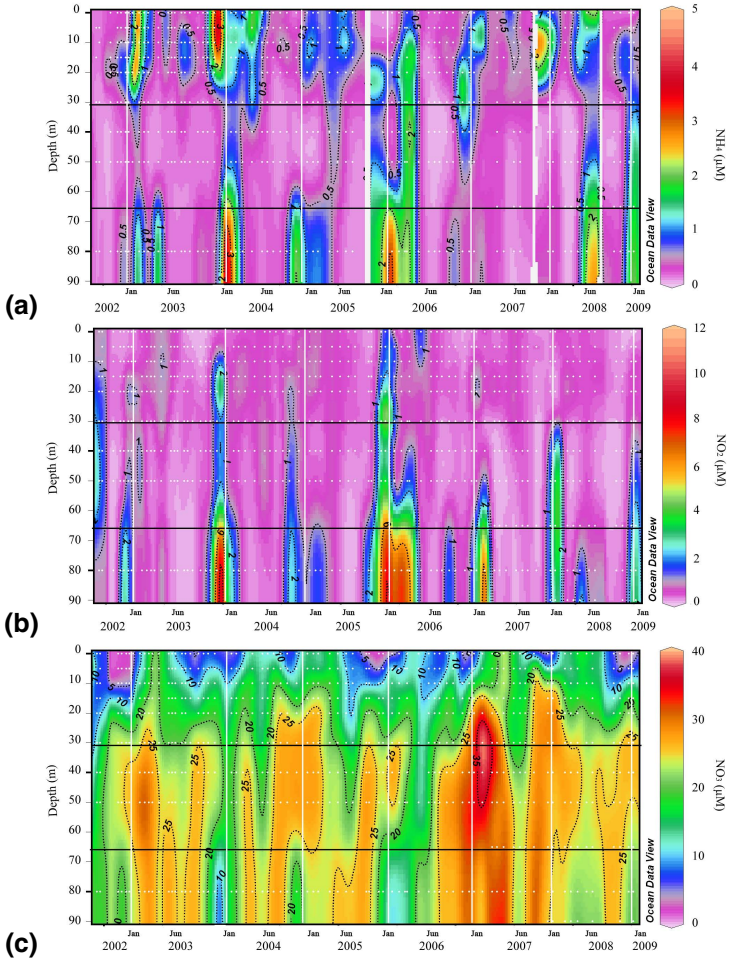

Fig. 4. Temporal variability of **(a)** ammonium, **(b)** nitrite and **(c)** nitrate concentration at Station 18 (August 2002 to date).

BGD
6, 6205–6247, 2009

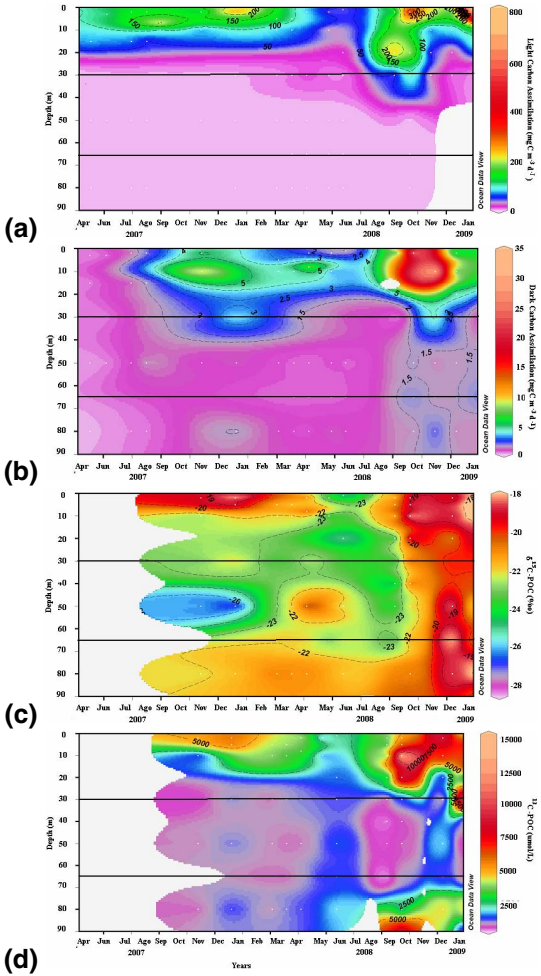

Fig. 5. Seasonal variation in autotrophic carbon fixation **(a)** photoautotrophic carbon assimilation **(b)** dark carbon assimilation; **(c)** natural C isotopic composition of POM and **(d)** POC concentration (data since April 2007).

BGD
6, 6205–6247, 2009

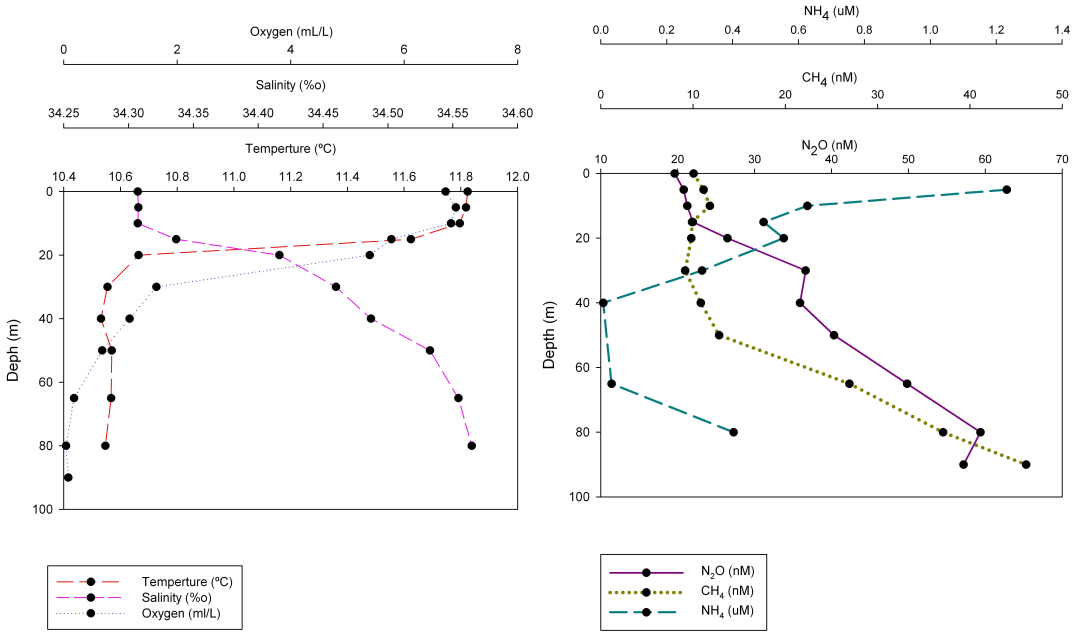

Fig. 6a. Profiles of hydrographic and oceanographic condition at the time experiment in a representative depth (80 m; B-layer) during the MI-LOCO cruise (January 2009) of: **(a)** dark carbon assimilation, **(b)** CH_4, and **(c)** N_2O cycling time course experiments under different treatments (control and ATU and GC7 amended incubation). The lines represent linear regressions.

BGD
6, 6205–6247, 2009

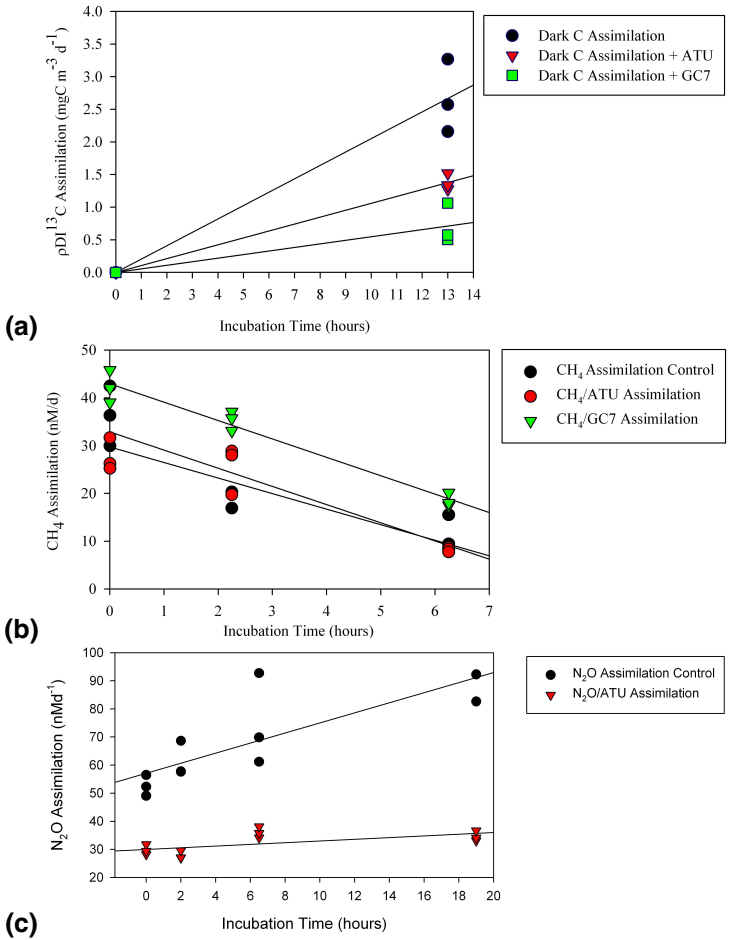

Fig. 6b. Continued.